Published in final edited form as:
J Mol Cell Cardiol. 2011 April ; 50(4): 662–669. doi:10.1016/j.yjmcc.2010.12.023.

Complex and rate-dependent beat-to-beat variations in Ca^{2+} transients of canine Purkinje cells

Young-Seon Lee[1], **Wen Dun**[2], **Penelope A. Boyden**[2], and **Eric A. Sobie**[1]

[1]Department of Pharmacology and Systems Therapeutics, Mount Sinai School of Medicine, New York, NY, USA

[2]Department of Pharmacology, Columbia University, New York, NY, USA

Abstract

Purkinje fibers play an essential role in transmitting electrical impulses through the heart, but they may also serve as triggers for arrhythmias linked to defective intracellular calcium (Ca^{2+}) regulation. Although prior studies have extensively characterized spontaneous Ca^{2+} release in nondriven Purkinje cells, little attention has been paid to rate-dependent changes in Ca^{2+} transients. Therefore we explored the behaviors of Ca^{2+} transients at pacing rates ranging from 0.125 to 3 Hz in single canine Purkinje cells loaded with fluo3 and imaged with a confocal microscope. The experiments uncovered the following novel aspects of Ca^{2+} regulation in Purkinje cells: 1) the cells exhibit a negative Ca^{2+}-frequency relationship (at 2.5 Hz, Ca^{2+} transient amplitude was 66 ± 6% smaller than that at 0.125 Hz); 2) sarcoplasmic reticulum (SR) Ca^{2+} release occurs as a propagating wave at very low rates but is localized near the cell membrane at higher rates; 3) SR Ca^{2+} load declines modestly (10 ± 5%) with an increase in pacing rate from 0.125 Hz to 2.5 Hz; 4) Ca^{2+} transients show considerable beat-to-beat variability, with greater variability occurring at higher pacing rates. Analysis of beat-to-beat variability suggests that it can be accounted for by stochastic triggering of local Ca^{2+} release events. Consistent with this hypothesis, an increase in triggering probability caused a decrease in the relative variability. These results offer new insight into how Ca^{2+} release is normally regulated in Purkinje cells and provide clues regarding how disruptions in this regulation may lead to deleterious consequences such as arrhythmias.

Keywords

Ca^{2+} transients; pacing rate; conduction system; Ca^{2+} sparks; Ca^{2+} waves

Corresponding Author: Eric Sobie, One Gustave Levy Place, Box 1215, New York, NY 10029, USA, Phone: 212 659 1706; FAX: 212 831 0114; eric.sobie@mssm.edu.

Disclosures None to declare.

Supplementary Materials Supplementary Figures associated with this manuscript illustrate: 1) the calculation of Ca^{2+} wave velocity (Figure S1); 2) the lack of Ca^{2+} wave propagation in a cell with SR Ca^{2+} release disabled (Figure S2); 3) analyses to determine whether Ca^{2+} transient amplitude on one beat influences the subsequent beat (Figure S3); and 4) additional calculations about how Ca^{2+} spark triggering may influence the rate dependence of COV (Figure S4).

Introduction

Purkinje fibers in heart are specialized networks of cells that play a critical role in electrical activity by rapidly conducting action potentials from the atrioventricular node to the ventricular endocardium [1]. Accordingly, research efforts have focused on determining the electrophysiological and conduction characteristics that allow them to fulfill this particular role.

Under pathological conditions, however, evidence suggests that spontaneous action potentials originating in the Purkinje network may serve as triggers for ventricular arrhythmias (eg. [2,3]). Moreover, this triggered activity has been linked to intracellular Ca^{2+} regulation, whereby spontaneous release of Ca^{2+} from the sarcoplasmic reticulum (SR) during diastole leads to inappropriate membrane depolarization when Ca^{2+} is extruded from the cell via the Na^{+}-Ca^{2+} exchanger [4,5]. Understanding, and potentially preventing, these triggered arrhythmias therefore requires greater knowledge of the mechanisms of Ca^{2+} regulation in cells from the Purkinje network.

Prior work has established that the coupling of electrical excitation to SR Ca^{2+} release in Purkinje cells exhibits important qualitative differences compared with ventricular myocytes [6,7]. In both cell types, Ca^{2+} entry through L-type Ca^{2+} channels triggers release of Ca^{2+} from SR stores, and intracellular Ca^{2+} transients reflect the contributions of both entry and release. Importantly, however, the extensive network of transverse (T) tubules in ventricular myocytes ensures that the pattern of SR Ca^{2+} release is relatively uniform throughout the cell [8,9]. Since Purkinje cells are largely devoid of T-tubules [10,11], SR Ca^{2+} release originates at the cell periphery where L-type Ca^{2+} channels in the cell membrane come in close contact with clusters of ryanodine receptors (RyRs) [4,7]. Spontaneous SR Ca^{2+} release in quiescent canine Purkinje cells has been extensively characterized and shown to consist of local Ca^{2+} sparks, slightly larger macrosparks or Ca^{2+} wavelets, and occasional propagating cell-wide Ca^{2+} waves [4,5,12]. Electrical stimuli applied to resting cells have been shown to induce Ca^{2+} waves which propagate transversely from the cell periphery to the core [5]. Much less is known, however, about how patterns of SR Ca^{2+} release change with pacing rate in periodically-stimulated Purkinje cells. The goal of this study, therefore, was to investigate rate-dependent changes in Ca^{2+} transients, with particular attention to potentially de-stabilizing patterns of Ca^{2+} release. We found that canine Purkinje cells exhibit a negative Ca^{2+}-frequency relationship, whereby large Ca^{2+} transients in the form of propagating Ca^{2+} waves occur at very low rates but only smaller, local events occur at higher rates. Moreover, we found, somewhat surprisingly, that Purkinje cells exhibit considerable inherent beat-to-beat variability in SR Ca^{2+} release, which can be accounted for by stochastic triggering of local Ca^{2+} release events.

Materials and Methods

Cell Isolation

Purkinje cells were enzymatically dispersed from the Purkinje fibers of the canine heart as previously described [10]. Briefly, Purkinje fibers were carefully dissected from RV and LV of canine hearts and subjected to enzyme incubation and dispersion. Purkinje cells studied here were isolated and did not show blebs or contraction bands.

Fluorescence Ca^{2+} imaging and solutions

Freshly isolated cells were loaded with the Ca^{2+}-sensitive indicator fluo-3 AM for 30 minutes, then placed in an experimental chamber and imaged with a 40 x oil immersion objective. Recordings of intracellular [Ca^{2+}] were obtained with a laser scanning confocal microscope (Zeiss LSM 510 Exciter) by exciting fluo-3 at 488 nm and recording

fluorescence above 505 nm. Cellular fluorescence was measured in line-scan mode at a rate of 4 ms per line, and only cells that did not show spontaneous contractions were selected for investigation. To reduce artifacts from contractile motion, the following steps were taken: 1) the scan line was oriented transversely; 2) the scan line was drawn as close to the center of the cell as possible without scanning a nucleus; 3) the glass bottom of the chamber was coated with laminin to improve cell attachment and reduce motion. For all Ca^{2+} imaging experiments cells were continually superfused with Tyrode's solution containing (in mM): NaCl 140, KCl 5.4, $CaCl_2$ 2, $MgCl_2$ 1, HEPES 10, glucose 10, pH 7.4. All experiments were performed at room temperature (22-24°C).

Electrical stimulation and Ca^{2+} transient recording

Purkinje cells were periodically stimulated by external field pulses applied through platinum electrodes located on opposite sides of the experimental chamber. Pacing cycle lengths ranged from 8 s to 0.25 s. To reduce the exposure of cells to laser light and allow for recordings over minutes, we configured the microscope to only scan during a brief period surrounding each electrical stimulus. For all recordings in this paper except those shown in Fig. 1, total recording time was reduced to about 170 ms (36 scan lines) for each Ca^{2+} transient. Among these 36 lines, 6 lines were obtained prior to electrical stimulation, and the remaining 30 lines defined the rising phase, peak, and initial declining phase of the Ca^{2+} transient. The spatial resolution was set to approximately 0.1 μm per pixel. In the experiment shown in Fig. 1, the total recording time was set about 300 ms to observe propagation of Ca^{2+} release into the cell core.

Image analysis of Ca^{2+} transients

To compute beat-to-beat changes in the response to electrical stimulation, Ca^{2+} transients were measured at three spatial regions: two sub-sarcolemmal (SSL) regions, defined as the 5 μm closest to the cell edges [12], and in the cell core. We observed that the resting fluorescence (F_0) prior to the initial stimulus was not uniform along the transversely-oriented scan line. Thus F_0 was calculated as a function of spatial location x, and Ca^{2+} transients were normalized on a pixel-by-pixel basis. F_0 was calculated before electrical stimulation commenced, and all subsequent Ca^{2+} transients were normalized to this value. This allowed us to observe changes in diastolic $[Ca^{2+}]$ caused by changes in pacing rate.

Ca^{2+} concentration calibration

To convert from normalized fluorescence to $[Ca^{2+}]$, we used the "pseudo-ratio" equation developed for single wavelength indicators [13]: $[Ca^{2+}] = KR/(K/[Ca^{2+}]_{rest} - R + 1)$, where K is the affinity of the indicator for calcium, and R is the normalized fluorescence (F/F_0). We set K = 0.7 μM, $[Ca^{2+}]_{rest}$ = 0.1 μM.

Caffeine application

To assess the SR Ca^{2+} load at a fixed pacing cycle length (PCL), 20 mM Caffeine was rapidly applied to a single cell after at least 10 beats at PCL= 8 s and 20 beats at PCL= 0.4 s. The solution change was timed so that caffeine reached the cell approximately when the next stimulus would have occurred. SR Ca^{2+} load was approximated as the peak normalized change in fluorescence ($\Delta F/F_0$) upon caffeine application [14]. Changes in fluorescence induced by caffeine were normalized to resting fluorescence (F_0) measured prior to electrical stimulation.

Statistics

Data are presented as mean ± s.e.m. Differences between groups were analyzed using a paired t test, with $p < 0.05$ considered statistically significant.

Results

Patterns of SR Ca^{2+} release are strongly rate-dependent

To understand rate-dependent changes in SR Ca^{2+} release in cardiac Purkinje cells, we recorded from periodically-stimulated cells using the line scan mode of the confocal microscope, with the scan line oriented in the transverse direction. Representative pseudo-images at two different rates are shown in Figure 1, with location on the y-axis and time on the x-axis. At an extremely low pacing rate (PCL = 8s; Fig. 1A), Ca^{2+} transients originated at the cell periphery (SSL) and then propagated into the cell core, exhibiting the V-shaped pattern typical of Ca^{2+} waves seen previously in myocytes lacking T-tubules [7,15-18]. Strikingly different behavior was observed when this cell was paced at a slightly higher rate (PCL = 4 s; Fig. 1B). In this case SSL Ca^{2+} transients were smaller than at PCL = 8 s, and little increase in Ca^{2+} was observed in the cell core, consistent with failed Ca^{2+} wave propagation. SSL and core Ca^{2+} transients averaged over 5 μm regions illustrate this difference (Figs. 1C and 1D), and a "time-to-target" analysis of Ca^{2+} wave velocity (Fig. 1E) indicated that successful propagation to the cell core at PCL = 8 s was faster than failed, local diffusion seen at PCL = 4 s (84.5 μm/s versus 44.1 μm/s). Moreover, the linear relationship between location and activation time at PCL = 8 s is consistent with regenerative Ca^{2+} wave propagation whereas the progressively longer delays seen at PCL = 4 s are consistent with passive Ca^{2+} diffusion. Similar results were seen in n=9 cells, with the transition from successful waves to failed waves occurring at PCL = 4.9 ± 0.35 s. Ca^{2+} waves propagating into the cell core were never observed in cells pre-treated with ryanodine and thapsigargin to block SR Ca^{2+} uptake (Supplementary Figure S2). Together these results indicate that at extremely low pacing rates, Ca^{2+} release occurs via the regenerative propagation of local release events, whereas at high pacing rates only local elevations in $[Ca^{2+}]$ and simple diffusion away from the cell periphery is observed.

Purkinje cells exhibit a negative $[Ca^{2+}]$-frequency relationship

To investigate the rate dependence of Purkinje cell Ca^{2+} transients more systematically, we progressively increased the pacing rate while recording the rising phase of the SSL Ca^{2+} transients at each rate. Figure 2 displays the amplitudes of 192 consecutive Ca^{2+} transients recorded in an individual cell at PCLs ranging from 6 s to 0.4 s. The blue and red dots represent SSL Ca^{2+} transient amplitudes recorded just under the cell membrane at the two edges of the cell. An increase in rate caused a progressive decrease in Ca^{2+} transient amplitude at both locations. Averaged Ca^{2+} transients from the two edges at three values of PCL are shown in Fig. 2, B-D. This result shows that the $[Ca^{2+}]$-frequency relationship in canine Purkinje cells is negative. Similar results were observed in *n*=7 cells. To our knowledge, this is the first such quantification of this relationship in this cell type.

Beat-to-beat variability persists at constant cycle length

An additional observation from Fig. 2 is the fact that, at each sub-sarcolemmal region, the Ca^{2+} transient amplitude at a given PCL fluctuates considerably from beat to beat. In this experiment, some of the variability may have been caused by transient effects due to a recent abrupt change in the pacing rate. To clarify this issue, we performed additional experiments in which we recorded many (> 65) consecutive Ca^{2+} transients at a few PCLs. Figure 3 shows, for three values of PCL, two sets of six consecutive SSL Ca^{2+} transients: the first obtained after 30 beats at that PCL, and the second after an additional 23 beats. These results demonstrate that beat-to-beat variability in local SSL Ca^{2+} transient amplitude persists in Purkinje cells, even during sustained pacing at a constant cycle length.

Relative variability of SSL Ca^{2+} transients is greater at higher pacing rates

Results in Figs. 2 and 3 suggest that beat-to-beat variability in local Ca^{2+} transient amplitude is substantial in Purkinje cells. Two issues that are not clear, however, are: 1) how does this variability depend on PCL? and 2) do beat to beat changes in amplitude show a regular pattern such as alternans? To address these questions, we performed two additional analyses. To quantify variability, Fig. 4A displays, as a function of PCL, the coefficient of variation (COV), i.e. the standard deviation of local Ca^{2+} transient amplitude divided by the mean amplitude at that PCL. COV increases as PCL decreases; i.e. fast pacing leads to a greater relative variability in local Ca^{2+} transient amplitude. Figure 4B shows a map of Ca^{2+} transient amplitude at the current beat ($\Delta F(N)$) versus Ca^{2+} transient amplitude on the subsequent beat ($\Delta F(N+1)$). At low rates, data points are located in the upper right of the map, indicating larger amplitudes at these rates, and are aggregated close to the line of identity, indicating relatively constant beat-to-beat amplitude. At high rates, data points fill the space around the line of identity, with no obvious pattern. To explore in more detail whether Ca^{2+} transient amplitude on one beat influences the next beat, we calculated temporal persistence, a measure that allows for robust detection of small alternans, even in the presence of noise [19]. Temporal persistence in our data, however, was less than 20% (Supplementary Figure S3), close to the values that can occur in completely random sequences. Together these results suggest that the amplitude of the N_{th} beat has little influence on the amplitude of the $(N+1)_{th}$ beat. Thus, faster pacing leads to greater variability in SSL Ca^{2+} transients, but unlike regular alternating patterns seen in ventricular myocytes [20], beat-to-beat patterns are highly irregular.

Pacing rate influences SR Ca^{2+} load

The smaller local Ca^{2+} transients observed with fast pacing in Purkinje cells may result, at least in part, from a smaller SR Ca^{2+} load. To assess this hypothesis, we rapidly applied 20 mM caffeine after pacing cells at a constant rate. Figure 5A and B demonstrate results from a single cell indicating that SR Ca^{2+} load, quantified as $\Delta F/F_0$ averaged across the cell width in response to caffeine, is slightly smaller at PCL = 0.4 s compared with PCL = 8 s. Fig. 5C presents a line-scan image from a different cell illustrating that caffeine causes increases in Ca^{2+} in both the SSL regions and the cell core. Summary results (n=10 cells) in Fig. 5D show the modest (10%) decrease in caffeine-induced $\Delta F/F_0$ at PCL = 0.4 s compared with PCL = 8 s. Although the change in SR Ca^{2+} load reached statistical significance ($p = 0.03$), the decrease in load from slow to fast pacing was considerably smaller than the decrease in SSL Ca^{2+} transient amplitude (66%, $n = 10$ cells). When expressed as changes in $\Delta[Ca^{2+}]$ rather than $\Delta F/F_0$, the mean data suggest that rapid pacing causes a 75% decrease in Ca^{2+} transient amplitude but only a 27% decrease in SR Ca^{2+} load. The results suggest, therefore, that mechanisms besides changes in SR Ca^{2+} load contribute to the negative Ca^{2+}-frequency relationship in these cells.

A simple mathematical model suggests a mechanism underlying beat-to-beat variability

How does beat-to-beat variability occur in Purkinje cells? Based on our results, we hypothesize that the number of RyR clusters, or Ca^{2+} release units (CRUs), contributing to each recorded local Ca^{2+} transient is relatively small, and stochastic effects may therefore dominate the observed variability. In accordance with this hypothesis, we propose a simple model of Ca^{2+} transient amplitude variability based on binomial statistics. We assume that, in the sub-sarcolemmal region near the cell membrane: 1) the confocal microscope records from a volume containing N CRUs (Fig. 6A); 2) the CRUs are triggered independently; and 3) the amplitudes of the Ca^{2+} sparks from the triggered CRUs are identical. If, with each electrical stimulus, the probability of triggering a spark from a CRU is p, then the probability that exactly k Ca^{2+} sparks are triggered on a given beat is described by the k^{th} term of the binomial distribution:

$$P(k)=\binom{N}{k}p^k(1-p)^{N-k} \quad (1)$$

If A is the amplitude of a Ca^{2+} spark, then the mean and coefficient of variation (COV) of Ca^{2+} transients recorded from the imaging volume are

$$\mu=A\cdot N\cdot p \quad (2)$$

$$COV=\sqrt{\frac{(1-p)}{N\cdot p}} \quad (3)$$

We sought to determine whether these predictions of mean Ca^{2+} transient amplitude (μ) and COV were consistent with our data. Since μ depends on the product $A{\cdot}N$ (Eq. 2), it follows that Ca^{2+} transient amplitude can be equally well-explained by a model with large A, small N, or one with small A, large N. In other words, based on mean amplitude alone, one cannot infer whether many CRUs are each producing small sparks, or few CRUs are each generating larger sparks. Beginning with μ obtained at PCL = 6 s, and assuming for simplicity that A does not depend on PCL, we determined the values of p at each PCL required to explain the Ca^{2+} transient mean amplitude data. Consistent with the above argument, Fig. 6C shows that results from a given cell could be equally well-fit by a model with N=35 (small) or one with N=300 (large). However, when we computed COV (Eq. 3) versus PCL for these parameters, we found that the model with N=35 fit the data well whereas the model with N=300 did not. Thus, the variability observed in our data can be explained by a simple model in which stochastic triggering of a limited number of release units contributes to the recorded signal.

Variability decreases with increasing triggering probability

Although the model based on binomial statistics is extremely simple, it allows us to generate predictions that can be tested experimentally. For instance, how does an increase in p affect COV? Fig 6D shows that with N=35, an increase in p causes a decrease in COV at all values of PCL (which can also be seen by inspecting Eq. 3). We tested this prediction by increasing extracellular $[Ca^{2+}]$ ($[Ca^{2+}]_o$) from 2 mM to 4 mM. An important aspect of this prediction is the fact that Ca^{2+} spark amplitude A, which would be expected to increase at greater $[Ca^{2+}]_o$, does not influence COV (Eq. 3). In these experiments, PCL was fixed at 800 ms, a middle value in our range of cycle lengths. Many consecutive Ca^{2+} transients were recorded with $[Ca^{2+}]_o$ = 2 mM (Fig. 7A), cells were perfused with $[Ca^{2+}]_o$ = 4 mM for 5 minutes while pacing continued, then recording was resumed at the same scan line. Fig. 7B shows that at $[Ca^{2+}]_o$ = 4 mM, Ca^{2+} transient amplitude increased, but the relative variability decreased at both edges of the cell, consistent with the model prediction. Summary data in Fig 7C show that COV decreased substantially (by 51 ± 11 %) and significantly ($p < 0.001$) with an increase in $[Ca^{2+}]_o$ from 2 mM to 4 mM.

Discussion

In this study, we have presented new results indicating how pacing rate influences the patterns of SR Ca^{2+} release observed in isolated, periodically-stimulated Purkinje cells. Electrical stimulation induced SSL Ca^{2+} release events which then propagated as Ca^{2+}

waves to the core. However, when cells were paced at rates above roughly 0.25 Hz, only smaller, local SSL transients occurred, and wave propagation failed. A further increase in pacing rate caused a further decline in Ca^{2+} transient amplitude, accompanied by a modest decrease in SR Ca^{2+} load. With repetitive stimulation, considerable Ca^{2+} transient amplitude variability was observed, without any obvious beat-to-beat pattern. A simple mathematical model and a straightforward test of model predictions suggest that this variability may result from stochastic effects due to a small number of Ca^{2+} release sites contributing to the measured signal.

Negative Ca^{2+}-frequency relationship

We observed, to our knowledge for the first time, that Ca^{2+} transient amplitude declines with increasing pacing rate in canine Purkinje cells, i.e. these cells exhibit a negative Ca^{2+}-frequency relationship. In 1981 Wasserstrom & Ferrier measured a negative relationship between contractile force and pacing frequency in canine Purkinje fibers [21] – our study complements and extends this prior result by documenting changes in the patterns of SR Ca^{2+} release at different frequencies. For instance, we found that Ca^{2+} waves propagating from the periphery to the core occurred at low pacing rates, consistent with prior studies performed in cells lacking T-tubules [4,7,15,17,22], whereas release only occurred in the subsarcolemmal region at higher rates. Although most ventricular myocytes from larger mammals show a positive Ca^{2+}-frequency relationship [14], some studies have suggested that this relationship is flat or negative in heart failure [23]. Since heart failure has been shown to lead to profound disruptions in the T-tubular system [24-26], an interesting question for future work is whether the loss of T-tubules per se causes changes in the Ca^{2+}-frequency relationship of mammalian heart cells.

Although we have observed that SR Ca^{2+} load is smaller at PCL = 0.4 s compared with PCL = 8 s, this decrease is relatively modest (10%) compared with the reduction in SSL Ca^{2+} transient amplitude (66%). Even after taking into account the roughly cubic relationship between load and release measured in ventricular myocytes [27], it seems likely that other mechanisms are required to explain the decrease in Ca^{2+} transient amplitude. While determining the mechanisms underlying the Ca^{2+}-frequency relationship was beyond the scope of this study, factors that may potentially contribute include: 1) decreased peak Ca^{2+} current at higher rates due to accumulating inactivation of L-type Ca^{2+} channels; 2) rate-dependent changes in transient outward current; and 3) greater refractoriness of the ryanodine receptor at higher rates. The last possibility is especially intriguing given: (1) the modest reduction in cellular SR Ca^{2+} load at high rates, and (2) the fact that dynamic local changes in SR $[Ca^{2+}]$ appear to control RyR refractoriness and recovery in ventricular muscle [28-30]. A potential explanation for the apparent discrepancy is that during fast pacing in Purkinje cells, Ca^{2+} has been taken into the SR by SERCA pumps but has not yet diffused to the junctions where it can be released. Measurements of local recovery of SR Ca^{2+} release [31] in Purkinje cells would be required to address this hypothesis. A second possibility is that control of RyR gating is fundamentally different in Purkinje cells, and a mechanism such as Ca^{2+}-dependent inactivation, which appears to play no role in the ventricle [32], contributes to refractoriness during rapid pacing. Future studies can explore these interesting possibilities.

Beat-to-beat variability

We originally expected that rapid pacing of Purkinje cells would result in regular beat-to-beat changes in SR Ca^{2+} release, i.e. Ca^{2+} transient alternans as have been observed in ventricular myocytes [20,33,34]. Sustained beat-to-beat variability in the absence of Ca^{2+} transient alternans, which we found instead, was therefore somewhat unanticipated. This result becomes less surprising, however, when one considers that the confocal microscope in

line-scan mode records from a small volume in the region near the cell membrane where Ca^{2+} entry and SR Ca^{2+} release occur. It therefore seems quite reasonable that the recorded Ca^{2+} transients reflect the triggering of a relatively small number of Ca^{2+} sparks.

Experiments performed in atrial [22] and ventricular myocytes [13] have similarly observed some beat-to-beat variability in SR Ca^{2+} release. Our analysis extends these previous observations by: 1) quantifying COV at different pacing rates, and 2) proposing a simple mathematical model to account for the experimental observations. Our model suggests that the increased relative variability at higher pacing rates may be a simple consequence of the negative force frequency relationship: i.e. a decrease in spark triggering probability p at higher rates causes an increase in variability. The model further allows us to conclude that if the decrease in mean Ca^{2+} transient amplitude μ were to occur by a different mechanism, for instance a decrease in spark amplitude A, then faster pacing could hypothetically be accompanied by either no change or an increase in COV (Supplementary Figure S4).

If variability indeed results from our proposed mechanism, it follows that an increase in p should decrease the variability. When we tested this prediction by increasing extracellular $[Ca^{2+}]$, a decrease in variability was observed (Fig. 7). These results therefore suggest that stochastic Ca^{2+} spark triggering may be sufficient to explain the beat-to-beat variability that we found. Moreover, the lack of a clear pattern in consecutive Ca^{2+} transient amplitudes (Fig. 4B and Supplementary Figure S3) additionally suggests that stochastic effects are the most important factor.

Implications for arrhythmogenesis

The negative Ca^{2+}-frequency relationship and the dependence of Ca^{2+} wave propagation on pacing rate have important implications for Ca^{2+}-triggered arrhythmias originating in the Purkinje system. Our results suggest that spontaneous propagating Ca^{2+} waves, which cause inappropriate membrane depolarization and can initiate arrhythmias [4,35] are more likely to occur during slow rather than fast pacing. However, our results with rapid caffeine application indicate that SR stores in the cell core remain loaded with Ca^{2+} during rapid pacing. Moreover, since fast pacing causes only a small decline in total cellular SR Ca^{2+} load, this suggests that the rapidly-paced Purkinje cells may retain the ability to generate propagating Ca^{2+} waves. These considerations may help explain why arrhythmias can be frequently initiated after a pause in pacing [36]. During rapid pacing, the SR remains filled with Ca^{2+} even though triggered Ca^{2+} transients are small. A brief pause may allow RyRs to recover from refractoriness and thereby increase the probability that a spontaneous local Ca^{2+} release event will trigger a regenerative Ca^{2+} wave. Future studies can use more sophisticated pacing protocols to explore this hypothesis. Although a thorough understanding of the arrhythmic potential of Purkinje cells will also require consideration of factors such as β-adrenergic stimulation and disease states, the results presented here provide an important baseline for understanding future work.

An unresolved question, however, is how highly variable behavior at the sub-cellular level, as observed here, may be either pro-arrhythmic or anti-arrhythmic within the cardiac syncytium. Because beat-to-beat changes in local Ca^{2+} transients appeared to be essentially random, we speculate that these effects will still be present in the multicellular environment, but, due to averaging, variability per se will not be pro-arrhythmic. Future studies will be required to address these important issues.

Study Limitations

Several limitations should be considered. One is that all Ca^{2+} transient recordings were performed at room temperature. Although changes in temperature will certainly have

quantitative effects on Ca^{2+} transient amplitude, this limitation is unlikely to influence the general trends that we observed. For instance, Boyden et al previously found that physiological temperature led to an increase in the frequency of Ca^{2+} release events, but comparable differences between healthy Purkinje cells and those that remained in the ischemic border zone [4,5]. A second limitation is our use of the non-ratiometric dye fluo-3. Because we converted from fluorescence to $[Ca^{2+}]$ using the pseudo-ratio equation which required us to assume diastolic $[Ca^{2+}]$, our absolute Ca^{2+} transient amplitudes should be interpreted cautiously. We should note, however, that this limitation will not affect our observations regarding the relative changes in Ca^{2+} transient amplitude, beat-to-beat variability, and SR Ca^{2+} load made using consecutive measurements in individual cells. Finally, our calculations of SR Ca^{2+} load, computed as peak $\Delta F/F_0$ upon application of 20 mM caffeine, should be considered semi-quantitative, especially given that large increases in intracellular $[Ca^{2+}]$ may cause partial saturation of the indicator. More precise estimates of load could be obtained using fluorescent indicators trapped in the SR or by integrating Na^+-Ca^{2+} exchange current in voltage-clamped cells.

Conclusions

In summary, our study provides new information regarding how pacing rate influences the patterns of SR Ca^{2+} release observed in canine Purkinje cells. We found that Ca^{2+} transients are larger at low versus high pacing rates. The decrease in local Ca^{2+} release during faster pacing was accompanied by an increase in beat-to-beat variability, which is potentially explained by a model in which stochastic triggering of a relatively small number of Ca^{2+} release units determines beat-to-beat changes. The results have implications both for normal Purkinje cell function and for potentially arrhythmogenic Ca^{2+} release that can occur in disease.

Supplementary Material

Refer to Web version on PubMed Central for supplementary material.

Acknowledgments

We would like to thank Frank Fabris for technical assistance. This work was supported by National Institutes of Health grants HL076230 (EAS) and HL67449 (PAB).

References

1. Boyden PA, Hirose M, Dun W. Cardiac Purkinje cells. Heart Rhythm. 2010; 7(1):127–35. [PubMed: 19939742]
2. Bogun F, Good E, Reich S, Elmouchi D, Igic P, Tschopp D, et al. Role of Purkinje fibers in post-infarction ventricular tachycardia. J Am Coll Cardiol. 2006; 48(12):2500–7. [PubMed: 17174189]
3. Cerrone M, Noujaim SF, Tolkacheva EG, Talkachou A, O'Connell R, Berenfeld O, et al. Arrhythmogenic mechanisms in a mouse model of catecholaminergic polymorphic ventricular tachycardia. Circ Res. 2007; 101(10):1039–48. [PubMed: 17872467]
4. Boyden PA, Pu J, Pinto J, Keurs HE. Ca^{2+} transients and Ca^{2+} waves in purkinje cells : role in action potential initiation. Circ Res. 2000; 86(4):448–55. [PubMed: 10700450]
5. Boyden PA, Barbhaiya C, Lee T, ter Keurs HE. Nonuniform Ca^{2+} transients in arrhythmogenic Purkinje cells that survive in the infarcted canine heart. Cardiovasc Res. 2003; 57(3):681–93. [PubMed: 12618230]
6. Dun W, Boyden PA. The Purkinje cell; 2008 style. J Mol Cell Cardiol. 2008; 45(5):617–24. [PubMed: 18778712]

7. Cordeiro JM, Spitzer KW, Giles WR, Ershler PE, Cannell MB, Bridge JH. Location of the initiation site of calcium transients and sparks in rabbit heart Purkinje cells. The J Physiol. 2001; 531(Pt 2): 301–14.
8. Song LS, Guatimosim S, Gomez-Viquez L, Sobie EA, Ziman A, Hartmann H, et al. Calcium biology of the transverse tubules in heart. Ann N Y Acad Sci. 2005; 1047:99–111. [PubMed: 16093488]
9. Brette F, Orchard C. T-tubule function in mammalian cardiac myocytes. Circ Res. 2003; 92(11): 1182–92. [PubMed: 12805236]
10. Boyden PA, Albala A, Dresdner KP Jr. Electrophysiology and ultrastructure of canine subendocardial Purkinje cells isolated from control and 24-hour infarcted hearts. Circ Res. 1989; 65(4):955–70. [PubMed: 2791230]
11. Di Maio A, Ter Keurs HE, Franzini-Armstrong C. T-tubule profiles in Purkinje fibres of mammalian myocardium. J Muscle Res Cell Motil. 2007; 28(2-3):115–21. [PubMed: 17572852]
12. Stuyvers BD, Dun W, Matkovich S, Sorrentino V, Boyden PA, ter Keurs HE. Ca^{2+} sparks and waves in canine purkinje cells: a triple layered system of Ca^{2+} activation. Circ Res. 2005; 97(1): 35–43. [PubMed: 15947247]
13. Cannell MB, Cheng H, Lederer WJ. Spatial non-uniformities in $[Ca^{2+}]_i$ during excitation-contraction coupling in cardiac myocytes. Biophysical journal. 1994; 67(5):1942–56. [PubMed: 7858131]
14. Bers, DM. Excitation–Contraction Coupling and Cardiac Contractile Force. 2. Dordrecht/Boston/ London: Kluwer Academic Publishers; 2001.
15. Haddock PS, Coetzee WA, Cho E, Porter L, Katoh H, Bers DM, et al. Subcellular $[Ca^{2+}]_i$ gradients during excitation-contraction coupling in newborn rabbit ventricular myocytes. Circ Res. 1999; 85(5):415–27. [PubMed: 10473671]
16. Kirk MM, Izu LT, Chen-Izu Y, McCulle SL, Wier WG, Balke CW, et al. Role of the transverse-axial tubule system in generating calcium sparks and calcium transients in rat atrial myocytes. The J Physiol. 2003; 547(Pt 2):441–51.
17. Brette F, Despa S, Bers DM, Orchard CH. Spatiotemporal characteristics of SR Ca^{2+} uptake and release in detubulated rat ventricular myocytes. J Mol Cell Cardiol. 2005; 39(5):804–12. [PubMed: 16198369]
18. Huser J, Lipsius SL, Blatter LA. Calcium gradients during excitation-contraction coupling in cat atrial myocytes. The J Physiol. 1996; 494(Pt 3):641–51.
19. Jia Z, Bien H, Entcheva E. Detecting space-time alternating biological signals close to the bifurcation point. IEEE Trans Biomed Eng. 2010; 57(2):316–24. [PubMed: 19695992]
20. Chudin E, Goldhaber J, Garfinkel A, Weiss J, Kogan B. Intracellular Ca^{2+} dynamics and the stability of ventricular tachycardia. Biophysical journal. 1999; 77(6):2930–41. [PubMed: 10585917]
21. Wasserstrom JA, Ferrier GR. Voltage dependence of digitalis afterpotentials, aftercontractions, and inotropy. Am J Physiol. 1981; 241(4):H646–53. [PubMed: 7315990]
22. Kockskamper J, Sheehan KA, Bare DJ, Lipsius SL, Mignery GA, Blatter LA. Activation and propagation of Ca^{2+} release during excitation-contraction coupling in atrial myocytes. Biophysical journal. 2001; 81(5):2590–605. [PubMed: 11606273]
23. Sipido KR, Stankovicova T, Flameng W, Vanhaecke J, Verdonck F. Frequency dependence of Ca^{2+} release from the sarcoplasmic reticulum in human ventricular myocytes from end-stage heart failure. Cardiovasc Res. 1998; 37(2):478–88. [PubMed: 9614502]
24. Louch WE, Mork HK, Sexton J, Stromme TA, Laake P, Sjaastad I, et al. T-tubule disorganization and reduced synchrony of Ca^{2+} release in murine cardiomyocytes following myocardial infarction. The J Physiol. 2006; 574(Pt 2):519–33.
25. Balijepalli RC, Lokuta AJ, Maertz NA, Buck JM, Haworth RA, Valdivia HH, et al. Depletion of T-tubules and specific subcellular changes in sarcolemmal proteins in tachycardia-induced heart failure. Cardiovasc Res. 2003; 59(1):67–77. [PubMed: 12829177]
26. Song LS, Sobie EA, McCulle S, Lederer WJ, Balke CW, Cheng H. Orphaned ryanodine receptors in the failing heart. Proc Natl Acad Sci U S A. 2006; 103(11):4305–10. [PubMed: 16537526]

27. Trafford AW, Diaz ME, Eisner DA. Coordinated control of cell Ca^{2+} loading and triggered release from the sarcoplasmic reticulum underlies the rapid inotropic response to increased L-type Ca^{2+} current. Circ Res. 2001; 88(2):195–201. [PubMed: 11157672]
28. Sobie EA, Dilly KW, dos Santos Cruz J, Lederer WJ, Jafri MS. Termination of cardiac Ca(2+) sparks: an investigative mathematical model of calcium-induced calcium release. Biophys J. 2002; 83(1):59–78. [PubMed: 12080100]
29. Terentyev D, Viatchenko-Karpinski S, Gyorke I, Volpe P, Williams SC, Gyorke S. Calsequestrin determines the functional size and stability of cardiac intracellular calcium stores: Mechanism for hereditary arrhythmia. Proc Natl Acad Sci U S A. 2003; 100(20):11759–64. [PubMed: 13130076]
30. Szentesi P, Pignier C, Egger M, Kranias EG, Niggli E. Sarcoplasmic reticulum Ca^{2+} refilling controls recovery from Ca^{2+}-induced Ca^{2+} release refractoriness in heart muscle. Circ Res. 2004; 95(8):807–13. [PubMed: 15388639]
31. Sobie EA, Song LS, Lederer WJ. Local recovery of Ca^{2+} release in rat ventricular myocytes. The J Physiol. 2005; 565(Pt 2):441–7.
32. Stevens SC, Terentyev D, Kalyanasundaram A, Periasamy M, Gyorke S. Intra-sarcoplasmic reticulum Ca^{2+} oscillations are driven by dynamic regulation of ryanodine receptor function by luminal Ca^{2+} in cardiomyocytes. The J Physiol. 2009; 587(Pt 20):4863–72.
33. Diaz ME, O'Neill SC, Eisner DA. Sarcoplasmic reticulum calcium content fluctuation is the key to cardiac alternans. Circ Res. 2004; 94(5):650–6. [PubMed: 14752033]
34. Pruvot EJ, Katra RP, Rosenbaum DS, Laurita KR. Role of calcium cycling versus restitution in the mechanism of repolarization alternans. Circ Res. 2004; 94(8):1083–90. [PubMed: 15016735]
35. Pogwizd SM, Schlotthauer K, Li L, Yuan W, Bers DM. Arrhythmogenesis and contractile dysfunction in heart failure: Roles of sodium-calcium exchange, inward rectifier potassium current, and residual beta-adrenergic responsiveness. Circ Res. 2001; 88(11):1159–67. [PubMed: 11397782]
36. Leclercq JF, Maisonblanche P, Cauchemez B, Coumel P. Respective role of sympathetic tone and of cardiac pauses in the genesis of 62 cases of ventricular fibrillation recorded during Holter monitoring. Eur Heart J. 1988; 9(12):1276–83. [PubMed: 3229422]

List of abbreviations

PCL	pacing cycle length
SSL	sub-sarcolemmal
RyR	ryanodine receptors
SR	sarcoplasmic reticulum
T-tubule	Transverse tubule
F_0	resting fluorescence
$\Delta F/F_0$	normalized change in fluorescence
COV	coefficient of variation
CRU	Ca^{2+} release unit
SERCA	sarco/endoplasmic reticulum Ca^{2+}-ATPase

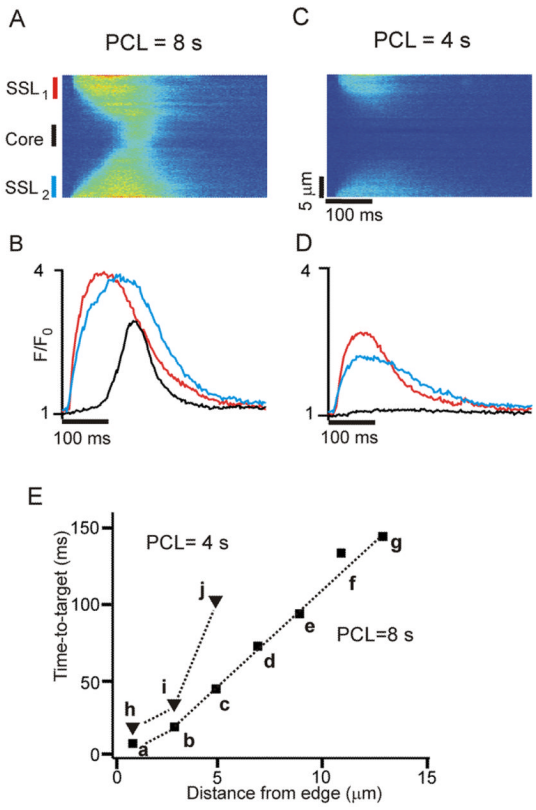

Figure 1.

Ca^{2+} waves occur at very low pacing rates; local subsarcolemmal (SSL) elevations in Ca^{2+} occur at higher pacing rates. **(A)** Space-time line scan image obtained at PCL = 8 s shows an early increase in $[Ca^{2+}]$ in SSL regions and a delayed increase in the core. **(B)** Local Ca^{2+} transients averaged over 5 μm at two SSL regions (red and blue) and in cell core (black), as indicated to the left of the image in **(A). (C)** and **(D)** Space-time image and local Ca^{2+} transients, respectively, obtained in the same cell at PCL = 4 s. Electrical stimulation induces elevations in Ca^{2+} only in the SSL regions. **(E)** Time-to-target plot of activation time versus distance from cell edge, with Ca^{2+} transients averaged over each 2 μm region.

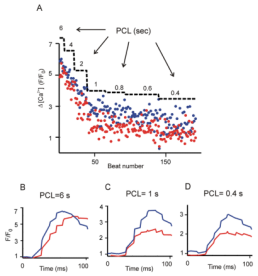

Figure 2.

Purkinje cells exhibit a negative $\Delta[Ca^{2+}]$ versus frequency relationship. A single Purkinje cell was paced with a protocol in which the PCL was progressively decreased and Ca^{2+} transients resulting from each stimulation were recorded. **(A)** Local SSL Ca^{2+} transients recorded from two edges of a cell. Amplitudes ($\Delta[Ca^{2+}]$= Peak−diastolic $[Ca^{2+}]$) calculated at the two SSL regions are denoted by red and blue circles. PCLs are superimposed as a staircase to mark each cycle length regime. **(B-D)** Averaged SSL $[Ca^{2+}]$ transients at PCL= 6 s **(B)**, 1 s **(C)**, 0.4 s **(D)**. All data were obtained at the same scan line in an individual cell.

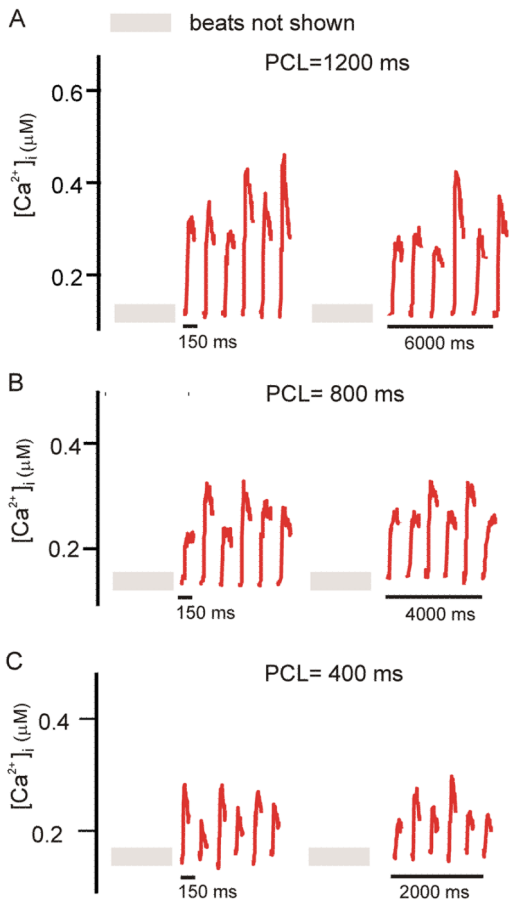

Figure 3.

Beat-to-beat variability in the local SSL persists with steady pacing. **(A), (B)**, and **(C)**, respectively, show SSL Ca^{2+} transients at PCL=1200, 800, and 400 ms. Each panel shows two sets of six consecutive Ca^{2+} transients, the first obtained after 29 stimuli, and the second obtained after 23 additional stimuli. At each PCL, variability in SSL Ca^{2+} transient amplitude persists.

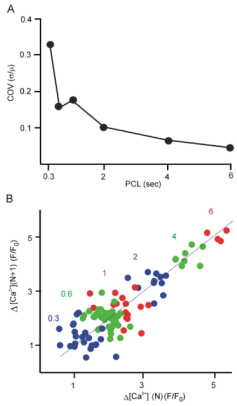

Figure 4.

Faster pacing leads to an increase in the normalized Ca^{2+} transient variability, but an irregular pattern from one beat to the next. **(A)** Coefficient of variation (COV) in SSL Ca^{2+} transient amplitude, computed in a single cell as the standard deviation divided by the mean, and plotted as a function of PCL. **(B)** Map of SSL Ca^{2+} transient amplitude on the current beat versus amplitude on the next beat at several different PCLs as indicated.

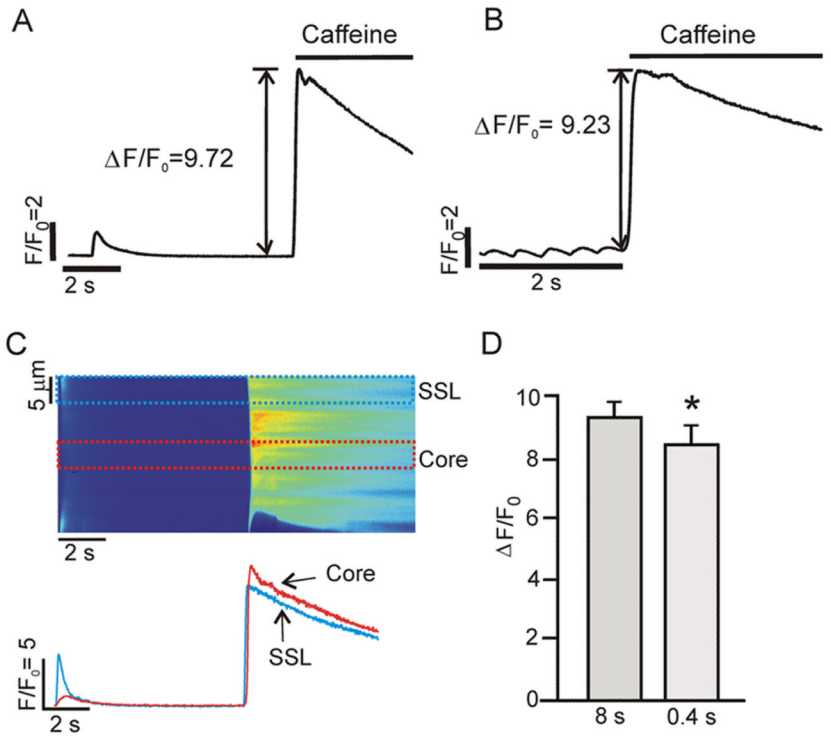

Figure 5.

SR Ca^{2+} load during slow and fast pacing. **(A)** Example showing the increase in cytosolic [Ca^{2+}] produced by rapid application of 20 mM caffeine after pacing at PCL = 8s. **(B)** Increase in cytosolic [Ca^{2+}] in the same cell after pacing at 0.4 s. **(C)** Space time image of the response to caffeine at PCL = 8 s (top), and SSL and core Ca^{2+} transients (5 μm average; bottom). **(D)** Pooled data (*n*=10 cells) illustrating that SR Ca^{2+} load, approximated as $\Delta F/F_0$ induced by 20 mM caffeine, is slightly lower at PCL = 0.4 s than at PCL = 8 s (8.41 ± 0.63 versus 9.30 ± 0.52; p = 0.03).

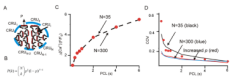

Figure 6.

Results of simple mathematical model. **(A)** Diagram of N Ca^{2+} release units (CRUs). During an action potential each unit has a probability of *p* to be triggered and generate an event with amplitude *A*. **(B)** Assuming that triggering from each CRU is an independent event, the k^{th} term of the binomial distribution describes the probability that *k* events are triggered. **(C)** Dots show the relationship between Ca^{2+} transient amplitude (averaged at one SSL of a cell) and PCL. The model can fit the data perfectly (dashed line) assuming either many release units, each with small amplitude (N=300), or fewer release units, each with larger amplitude (N=35). **(D)** COV data (black dots) from the same cell were compared with model results of N=35 (black solid line), N=300 (black dashed line) and N=35 with a 50% increased probability *p* (blue dashed line).

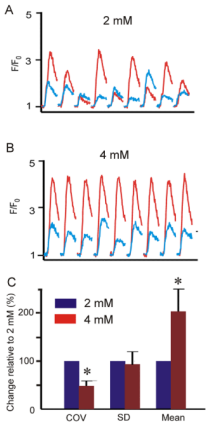

Figure 7.

An increase in triggering of Ca^{2+} release causes a decrease in relative Ca^{2+} transient variability. **(A)** $[Ca^{2+}]$ transients at two SSL regions with $[Ca^{2+}]_o$ = 2 mM. **(B)** $[Ca^{2+}]$ transients measured from the same locations in the same cell with $[Ca^{2+}]_o$ = 4 mM. **(C)** Pooled data (*n*=6 cells) illustrating that increasing $[Ca^{2+}]_o$ causes a significant (p = 0.005) increase in mean SSL Ca^{2+} transient amplitude and a significant (p < 0.001) decrease in COV. Average COV at 4 mM is 49 ± 11% of the value at 2 mM. For these statistical comparisons, we treated the two SSL regions in each cell as independent events such that *n*=6 cells generated a total of *n*=12 data pairs for comparison.